

# Regioselectivity in the Chemical Reactions between Molecules and Protons: A Quantum Fluid Density Functional Study

P. K. Chattaraj\* and B. Maiti

Department of Chemistry, Indian Institute of Technology, Kharagpur - 721 302, India

Received: April 29, 2003; In Final Form: November 18, 2003

Proton–molecule collisions mimicking various chemical reactions are studied within a quantum fluid density functional framework. The regioselectivity of a proton attack is clearly delineated through the dynamic hardness and polarizability profiles. A time-dependent version of the HSAB principle is found to be operative.

## I. Introduction

Collision processes between different atoms and molecules with protons have seen an upsurge of interest in recent years<sup>1,2</sup> because such processes are very important in nuclear physics and astrophysics. Theoretical studies on collision dynamics of one-electron,<sup>3–5</sup> two-electron,<sup>6–11</sup> and quasi-one-electron systems<sup>12,13</sup> and experimental works<sup>14,15</sup> ranging from one to many-electron systems are well-studied. A chemical reaction can be explained by a collision process. In a chemical reaction, reactants collide with each other to form product. Among all of the chemical reactions, ion–molecule reactions play an important role in various chemical systems<sup>16</sup> and are especially important in the chemistry governing molecule formation in dense interstellar clouds.<sup>17</sup> Because of the presence of hydrogen in the interstellar medium, many of these reactions involve proton transfer between various bases. All atoms and molecules can be considered to be bases because all neutral species are able to bind a proton. Ion–molecule reactions are governed by the famous hard–soft acid–base (HSAB) principle<sup>18–20</sup> given by R. G. Pearson. According to this principle,<sup>18–21</sup> “hard acids prefer to coordinate with hard bases and soft acids to soft bases for both their thermodynamic and kinetic properties.” Pearson<sup>22</sup> gives another important hardness-related principle, viz., the maximum hardness principle (MHP)<sup>18,23,24</sup> that states that<sup>23</sup> “there seems to be a rule of nature that molecules arrange themselves so as to be as hard as possible.” The HSAB principle demands the validity of the maximum hardness principle in various physical and chemical processes.<sup>25</sup> On the basis of the inverse relationship<sup>26</sup> between hardness and polarizability, a minimum polarizability principle (MPP)<sup>27</sup> has been proposed that states that “the natural direction of evolution of any system is toward a state of minimum polarizability.”

Theoretical calculation of hardness and polarizability for atoms, ions, radicals, molecules, and clusters are performed using ab initio SCF,<sup>25,28</sup> DFT,<sup>29</sup> coupled cluster,<sup>30</sup> and other theories, but most of these calculations are restricted to the ground state. Very little work<sup>31</sup> has been done to calculate the hardness and polarizability of chemical systems in excited electronic states. Density functional theory (DFT)<sup>20,32</sup> has been quite successful in the calculation of the hardness and polarizability of different chemical reactions. The HSAB principle has been analyzed in light of the principles of maximum hardness and minimum polarizability by making use of two important

aspects of DFT, viz., time-dependent (TD) DFT<sup>33</sup> and excited-state DFT.<sup>34</sup> There is no general excited-state DFT except for some special cases such as in states that are of lowest energy for a given symmetry class<sup>35</sup> and for two-state ensembles.<sup>36</sup>

For a system comprising  $N$  electrons in the field of one or more fixed nuclei that generate an external potential  $v(\vec{r})$ , the curvature of the plot representing the change in the electronic energy  $E$  with the number of electrons  $N$  gives us the hardness, viz.,

$$\eta = \frac{1}{2} \left( \frac{\partial^2 E}{\partial N^2} \right)_{v(\vec{r})} \quad (1)$$

and equivalently hardness can be expressed as<sup>37</sup>

$$\eta = \frac{1}{N} \int \int \eta(\vec{r}, \vec{r}') f(\vec{r}') \rho(\vec{r}) d\vec{r} d\vec{r}' \quad (2)$$

where  $f(\vec{r})$  is the Fukui function<sup>38</sup> and  $\eta(\vec{r}, \vec{r}')$  is the hardness kernel given by

$$\eta(\vec{r}, \vec{r}') = \frac{1}{2} \frac{\delta^2 F[\rho]}{\delta \rho(\vec{r}) \delta \rho(\vec{r}')} \quad (3)$$

in terms of the Hohenberg–Kohn–Sham universal functional of DFT.<sup>32</sup> The wave function of an  $N$ -particle system is completely characterized by  $N$  and  $v(\vec{r})$ . Whereas  $\eta$  measures the response of the system when  $N$  changes at fixed  $v(\vec{r})$ , polarizability ( $\alpha$ ) plays the same role for varying  $v(\vec{r})$  at constant  $N$ .

According to MHP and MPP, the system becomes softer, more polarizable, and more reactive on electronic excitation. These principles are valid in the cases of atoms,<sup>39</sup> ions,<sup>31</sup> and molecules<sup>40</sup> for the lowest-energy state of a particular symmetry and different complexions of a two-state ensemble. In this paper, we study the time evolution of various reactivity parameters such as the hardness and polarizability associated with a collision process between a proton and various homonuclear and heteronuclear diatomic molecules in their ground and excited electronic states. According to the HSAB principle, a proton, which is a hard acid, is expected to bind those systems that are in their ground states, where they are the hardest, and the binding affinity would keep on decreasing with electronic excitations. Here we verify this principle using time-dependent density functional theory (TDDFT) and excited-state density functional theory (DFT).

\* Corresponding author. E-mail: pkc@chem.iitkgp.ernet.in.

The present work reports different chemical reactions  $F_2 + H^+ \rightarrow HF_2^+$ ,  $N_2 + H^+ \rightarrow HN_2^+$ ,  $CO + H^+ \rightarrow HOC^+ + HCO^+$ ,  $HF + H^+ \rightarrow H_2F^+ + HFH^+$ , and  $BF + H^+ \rightarrow HFB^+ + HBF^+$ . Both homonuclear diatomics ( $F_2$  and  $N_2$ ) and heteronuclear diatomics ( $CO$ ,  $HF$ , and  $BF$ ) are considered in both the ground and first excited electronic states. The reactions involving heteronuclear molecules are specifically chosen to test the regioselectivity in a reaction involving a multiple-site molecule in both its ground and first excited electronic states. The theoretical background of the present work is provided in section II. Section III contains the numerical details, and the results and discussion are given in section IV. Finally, section V presents some concluding remarks.

## II. Theoretical Background

According to DFT, the single-particle density  $\rho(\vec{r}, t)$  contains all of the information of the system, and the total energy attains the minimum value for the true  $\rho(\vec{r})$ . A time-dependent (TD) version of DFT has also been shown to be uniquely invertible up to an additive TD function in the potential. This TDDFT strengthens the quantum fluid dynamics (QFD), which describes the dynamics of a quantum system in terms of the flow of a probability fluid associated with the probability density  $\rho(\vec{r}, t)$  and the current density  $\vec{j}(\vec{r}, t)$ . The time evolution of these two quantities is governed by two basic QFD equations, viz., the equation of continuity

$$\frac{\partial \rho}{\partial t} + \nabla \cdot (\rho \nabla \xi) = 0 \quad (4a)$$

and the equation of motion

$$\frac{\partial \xi}{\partial t} + \frac{1}{2}(\nabla \xi)^2 + \frac{\delta G[\rho]}{\delta \rho} + \int \frac{\rho(\vec{r}', t)}{|\vec{r} - \vec{r}'|} d\vec{r}' + v_{\text{ext}}(\vec{r}, t) = 0 \quad (4b)$$

where  $\xi$  is the velocity potential. The universal functional  $G[\rho]$  comprises kinetic and exchange correlation energy functionals, and  $v_{\text{ext}}(\vec{r}, t)$  is the external potential. Equations 4a and 4b can be written legitimately in 3-D space using the TDDFT;<sup>33</sup> accordingly, a 3-D complex-valued hydrodynamical function  $\phi(\vec{r}, t)$  can be defined in the following polar form within an irrotational approximation as

$$\phi(\vec{r}, t) = \rho(\vec{r}, t)^{1/2} \exp(i\xi(\vec{r}, t)) \quad (5a)$$

$$\rho(\vec{r}, t) = |\phi(\vec{r}, t)|^2 \quad (5b)$$

$$\vec{j}(\vec{r}, t) = [\phi_{\text{re}} \nabla \phi_{\text{im}} - \phi_{\text{im}} \nabla \phi_{\text{re}}] = \rho \nabla \xi \quad (5c)$$

It may be noted that  $\phi(\vec{r}, t)$  is the wave function for a one-electron system only. However, it provides  $\rho(\vec{r}, t)$  and  $\vec{j}(\vec{r}, t)$  (vide eqs 5a–c) for all systems, albeit with an irrotational velocity field that may cause trouble in obtaining proper Bohm trajectories with vortices.

A quantum fluid density functional theory (QFDFT) was developed<sup>10,41,42</sup> to study the time evolution of  $\phi(\vec{r}, t)$  by combining eqs 4a and 4b to generate the following generalized nonlinear Schrödinger equation (GNLSE):

$$\left[ -\frac{1}{2}\nabla^2 + v_{\text{eff}}(\vec{r}, t) \right] \phi(\vec{r}, t) = i \frac{\partial \phi(\vec{r}, t)}{\partial t} \quad i = \sqrt{-1} \quad (6)$$

In QFDFT, the dynamics of an  $N$ -electron system is studied<sup>10,41</sup> in terms of the behavior of  $N$  noninteracting particles moving under the influence of an effective potential field given by

$$v_{\text{eff}}(\vec{r}, t) = \frac{\delta T_{\text{NW}}}{\delta \rho} + \frac{\delta E_{\text{xc}}}{\delta \rho} + \int \frac{\rho(\vec{r}', t)}{|\vec{r} - \vec{r}'|} d\vec{r}' + v_{\text{ext}}(\vec{r}, t) \quad (7)$$

where  $T_{\text{NW}}$  and  $E_{\text{xc}}$  denote the non-Weizsäcker parts of the kinetic energy and exchange correlation energy functionals, respectively.

To construct the effective potential (eq 7) of eq 6, we need  $T_{\text{NW}}$ ,  $E_{\text{xc}}$ , and  $v_{\text{ext}}(\vec{r}, t)$ . The explicit form for  $E_{\text{xc}}$  is taken as

$$E_{\text{xc}}[\rho] = E_{\text{x}}[\rho] + E_{\text{c}}[\rho] \quad (8a)$$

where  $E_{\text{x}}[\rho]$  is the Dirac exchange functional modified in the spirit of Becke's functional<sup>43</sup> as follows:<sup>44</sup>

$$E_{\text{x}}[\rho] = -C_k \left[ \int \rho^{4/3} d\vec{r} + \int \frac{\rho^{4/3}}{1 + (r^2 \rho^{2/3} / 0.0244)} d\vec{r} \right] \quad C_k = \left( \frac{3}{4\pi} \right) (3\pi^2)^{1/3} \quad (8b)$$

$E_{\text{c}}[\rho]$  is a Wigner-type parametrized correlation energy functional given by<sup>45</sup>

$$E_{\text{c}}[\rho] = - \int \frac{\rho}{9.81 + 21.437 \rho^{-1/3}} d\vec{r} \quad (8c)$$

For the study of the collision process, the whole scattering system is considered to be a supermolecule, and the corresponding kinetic energy functional comprises two parts:<sup>10,41,46</sup>

$$T[\rho] = T_{\text{at}}[\rho] + T_{\text{mol}}[\rho] \quad (9a)$$

where the atomic part  $T_{\text{at}}[\rho]$  is taken as<sup>44,46</sup>

$$T_{\text{at}}[\rho] = \frac{1}{8} \int \frac{\nabla \rho \cdot \nabla \rho}{\rho} d\vec{r} + C_k \int \rho^{5/3} d\vec{r} - a(N) \lambda \int \frac{\rho^{4/3}/r}{1 + r \rho^{1/3}} d\vec{r} \quad (9b)$$

$$C_k = \left( \frac{3}{10} \right) (3\pi^2)^{2/3}; \lambda = 30 \left( \frac{3}{\pi} \right)^{1/3} \quad (9c)$$

$$a(N) = a_0 + a_1 N^{-1/3} + a_2 N^{-2/3}$$

$$a_0 = 0.1279, a_1 = 0.1811, a_2 = -0.0819 \quad (9d)$$

and  $T_{\text{mol}}[\rho]$  is given by<sup>41</sup>

$$T_{\text{mol}}[\rho] = \iint \frac{1}{N^2} \left[ \frac{1}{R^{12}} - \left( \frac{N}{10} \right)^{14} R^2 \exp(-0.8R) \right] \rho(\vec{r}) \rho(\vec{r}') d\vec{r} d\vec{r}' \quad (9e)$$

where  $R$  is the distance of the proton from the origin of the coordinate system, appearing as a parameter. It may, however, be noted that although  $T_{\text{mol}}[\rho]$  exhibits several acceptable and required characteristics<sup>41</sup> its inclusion is essentially ad hoc in nature.

The form for  $v_{\text{ext}}(\vec{r}, t)$  is taken as

$$v_{\text{ext}}(\vec{r}, t) = - \frac{Z_1}{|R_1(t) - \vec{r}|} - \frac{Z_2}{|R_2(t) - \vec{r}|} - \frac{Z_3}{|R_3(t) - \vec{r}|} \quad (10)$$

where  $R_1, R_2, R_3$  and  $Z_1, Z_2, Z_3$  are the radius vectors and atomic numbers of each atom of the target (molecule) and the projectile ( $H^+$ ), respectively. The target (molecule) has two nuclei. The

origin of the coordinate system is fixed on one of the target nuclei or between the two target nuclei and the position of the projectile is determined by a Coulomb trajectory.<sup>1</sup>

The time-dependent energy quantity,  $E(t)$ , can be defined<sup>33,47,48</sup> as the following density functional

$$E(t) = \frac{1}{2} \int \rho(\vec{r}, t) |\nabla \xi|^2 d\vec{r} + T[\rho] + E_{xc}[\rho] + \frac{1}{2} \int \int \frac{\rho(\vec{r}, t) \rho(\vec{r}', t)}{|\vec{r} - \vec{r}'|} d\vec{r} d\vec{r}' + \int v_{\text{ext}}(\vec{r}, t) \rho(\vec{r}, t) d\vec{r} \quad (11)$$

where the first term represents the macroscopic kinetic energy that vanishes for a state with zero current density, for example, in the ground state of a system.

To follow the hardness dynamics using eq 2, the Fukui function is modeled as follows<sup>38</sup>

$$f(\vec{r}) = \frac{s(\vec{r})}{\int s(\vec{r}) d\vec{r}} \quad (12a)$$

where the local softness  $s(\vec{r})$  is taken as<sup>49</sup>

$$s(\vec{r}) = \frac{\delta(\vec{r} - \vec{r}')}{2\eta(\vec{r}, \vec{r}')} \quad (12b)$$

The hardness kernel  $\eta(\vec{r}, \vec{r}')$  (eq 3) is calculated using the following local form<sup>46</sup> for  $F(\rho)$

$$F[\rho] = T^{\text{local}}[\rho] + V_{\text{ee}}^{\text{local}}[\rho] \quad (12c)$$

where the local kinetic energy<sup>44</sup> and electron–electron repulsion energy<sup>50</sup> are taken as

$$T^{\text{local}}[\rho] = C_k \int \rho^{5/3} d\vec{r} + C_x \int \frac{\rho^{4/3}/r}{1 + \frac{r\rho^{1/3}}{0.043}} d\vec{r} \quad (12d)$$

and

$$V_{\text{ee}}^{\text{local}}[\rho] = 0.7937(N-1)^{2/3} \int \rho^{4/3} d\vec{r} \quad (12e)$$

These local functionals are used because of the simplicity of the calculation of the second-order functional derivative (eq 3) and the associated Fukui function within this local model.<sup>45</sup>

The TD polarizability is written as

$$\alpha(t) = \frac{|D_{\text{ind}}^z(t)|}{|\mathcal{T}_z(t)|} \quad (13a)$$

where  $D_{\text{ind}}^z(t)$  is the electronic part of the induced dipole moment given as

$$D_{\text{ind}}^z(t) = \int z\rho(\vec{r}, t) d\vec{r} \quad (13b)$$

and  $\mathcal{T}_z(t)$  is the  $z$  component of the external coulomb field due to the incoming proton.

### III. Numerical Details

The GNLSE (eq 6) is solved numerically using a leapfrog-type finite difference scheme, and an alternating direction-implicit (ADI) method is employed to generate the density at the second time step from the input density, which is required for the leapfrog scheme to start. The azimuthal symmetry of the physical system allows us to integrate analytically over 0

$\leq \tilde{\phi} \leq 2\pi$  in a cylindrical polar coordinate  $(\tilde{\rho}, \tilde{\phi}, z)$  system. Equation 6 is transformed as

$$\left\{ \left( \frac{3}{4x^3} \right) \frac{\partial y}{\partial x} - \left( \frac{1}{4x^2} \right) \frac{\partial^2 y}{\partial x^2} - \frac{\partial^2 y}{\partial z^2} \right\} - \left( \frac{1}{x^4} - 2v_{\text{eff}} \right) y = 2i \frac{\partial y}{\partial t} \quad (14a)$$

where

$$y = \tilde{\rho}\phi \quad (14b)$$

and

$$\tilde{\rho} = x^2 \quad (14c)$$

The impact parameter and the initial velocity of the projectile are 0.1 and 1.0 a.u. respectively. A detailed discussion of the numerical solution can be found elsewhere.<sup>41</sup> The 4-31G double- $\zeta$  ground states as well as the excited states of  $\text{F}_2$ ,  $\text{N}_2$ ,  $\text{CO}$ ,  $\text{HF}$ , and  $\text{BF}$  are taken from Snyder and Basch.<sup>51</sup> Only singlet electronic states are considered in the present work.

### IV. Results and Discussions

The time evolution of different reactivity parameters such as hardness and polarizability are discussed for different chemical reactions both in ground and excited electronic states. All quantities are in atomic units. Features touching the uppermost line of the rectangular box in the figures imply that they have been truncated there.

The density profiles of the  $\text{N}_2$  and  $\text{F}_2$  molecules in their ground (respective electronic configurations:  $(\sigma_g 1s)^2 (\sigma_u 1s)^2 (\sigma_g 2s)^2 (\sigma_u 2s)^2 (\pi_u 2p)^4 (\sigma_g 2p)^2$ ,  $(\sigma_g 1s)^2 (\sigma_u 1s)^2 (\sigma_g 2s)^2 (\sigma_u 2s)^2 (\sigma_g 2p)^2 (\pi_u 2p)^4 (\pi_g 2p)^4$ ) and first excited (respective electronic configurations:  $(\sigma_g 1s)^2 (\sigma_u 1s)^2 (\sigma_g 2s)^2 (\sigma_u 2s)^2 (\pi_u 2p)^4 (\sigma_g 2p) (\pi_g 2p)$ ,  $(\sigma_g 1s)^2 (\sigma_u 1s)^2 (\sigma_g 2s)^2 (\sigma_u 2s)^2 (\sigma_g 2p)^2 (\pi_u 2p)^4 (\pi_g 2p)^3 (\sigma_u 2p)$ ) electronic states are presented as Supporting Information. The density profiles are symmetric at both of the nuclei in both electronic states of all of the molecules. The density decreases at the nuclear sites, but spreads out more as one goes radially away from the nuclei in the first excited electronic states of all of the molecules.

During protonation, hardness would be maximized and polarizability would be minimized in the neighborhood of the nuclei, and they would be symmetric in both sets of electronic states of  $\text{N}_2$  and  $\text{F}_2$  molecules, which is what is precisely obtained in the present work as depicted in Figures 1a and b and 2a and b, respectively. In the encounter regime,  $\eta$  becomes very large because of rapid charge oscillations because the electron density gets shared by all of the nuclei. Hardness becomes exceptionally large at the point of the closest approach of the two nuclei owing to the coulomb singularity. Perhaps a better trajectory for the nuclear motion would remedy this problem. Being softer and more polarizable, the first excited electronic state exhibits lower  $\eta_{\text{max}}$  and higher  $\alpha_{\text{min}}$  values when compared to the corresponding values for the ground state. Therefore, excited-state  $\text{N}_2$  and  $\text{F}_2$  molecules are more reactive than ground-state  $\text{N}_2$  and  $\text{F}_2$  molecules.

The density profiles of  $\text{HF}$ ,  $\text{BF}$ , and  $\text{CO}$  molecules in their ground (respective electronic configurations:  $(1\sigma)^2 (2\sigma)^2 (3\sigma)^2 (1\pi)^4 (1\sigma)^2 (2\sigma)^2 (3\sigma)^2 (4\sigma)^2 (1\pi)^4 (5\sigma)^2$ ,  $(1\sigma)^2 (2\sigma)^2 (3\sigma)^2 (4\sigma)^2 (1\pi)^4 (5\sigma)^2$ ) and first excited (respective electronic configurations:  $(1\sigma)^2 (2\sigma)^2 (3\sigma)^2 (1\pi)^3 (4\sigma)$ ,  $(1\sigma)^2 (2\sigma)^2 (3\sigma)^2 (4\sigma)^2 (1\pi)^4 (5\sigma) (2\pi)$ ,  $(1\sigma)^2 (2\sigma)^2 (3\sigma)^2 (4\sigma)^2 (1\pi)^4 (5\sigma) (2\pi)$ ) electronic states are presented as Supporting Information. Electron densities<sup>51</sup> are centered around the H and F nuclei in  $\text{HF}$ , around B and F nuclei in  $\text{BF}$ , and around C and O nuclei

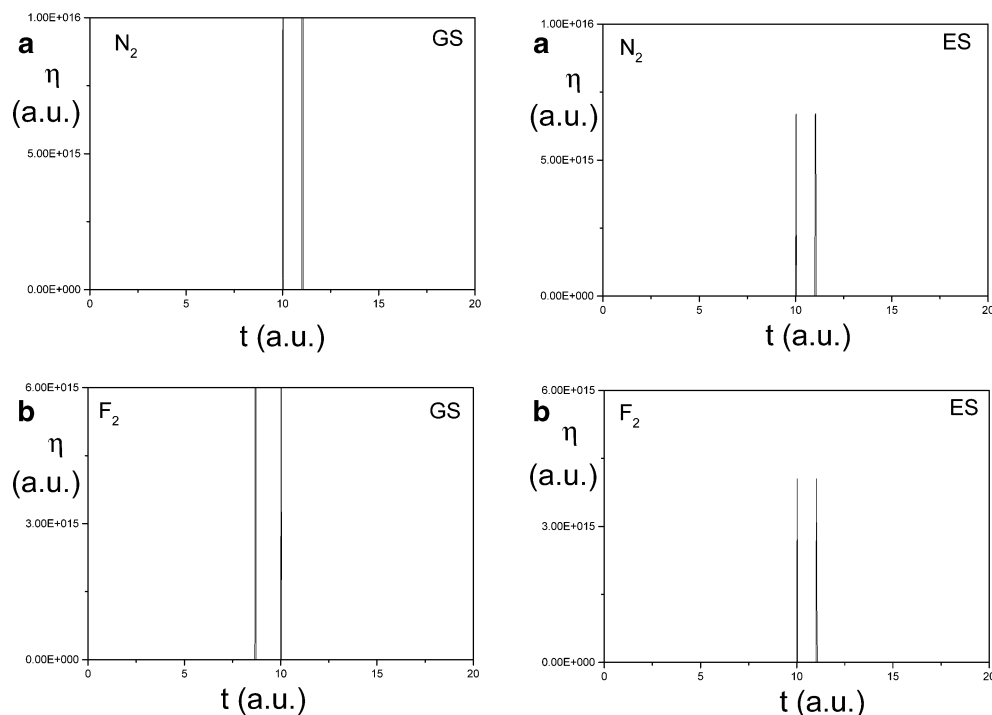


**Figure 1.** (a, left) Time (a.u.) evolution of hardness ( $\eta$ , a.u.) during a collision process between a nitrogen molecule in its ground state and a proton. (a, right) Time (a.u.) evolution of hardness ( $\eta$ , a.u.) during a collision process between a nitrogen molecule in its first excited state and a proton. (b, left) Time (a.u.) evolution of hardness ( $\eta$ , a.u.) during a collision process between a fluorine molecule in its ground state and a proton. (b, right) Time (a.u.) evolution of hardness ( $\eta$ , a.u.) during a collision process between a fluorine molecule in its first excited state and a proton.

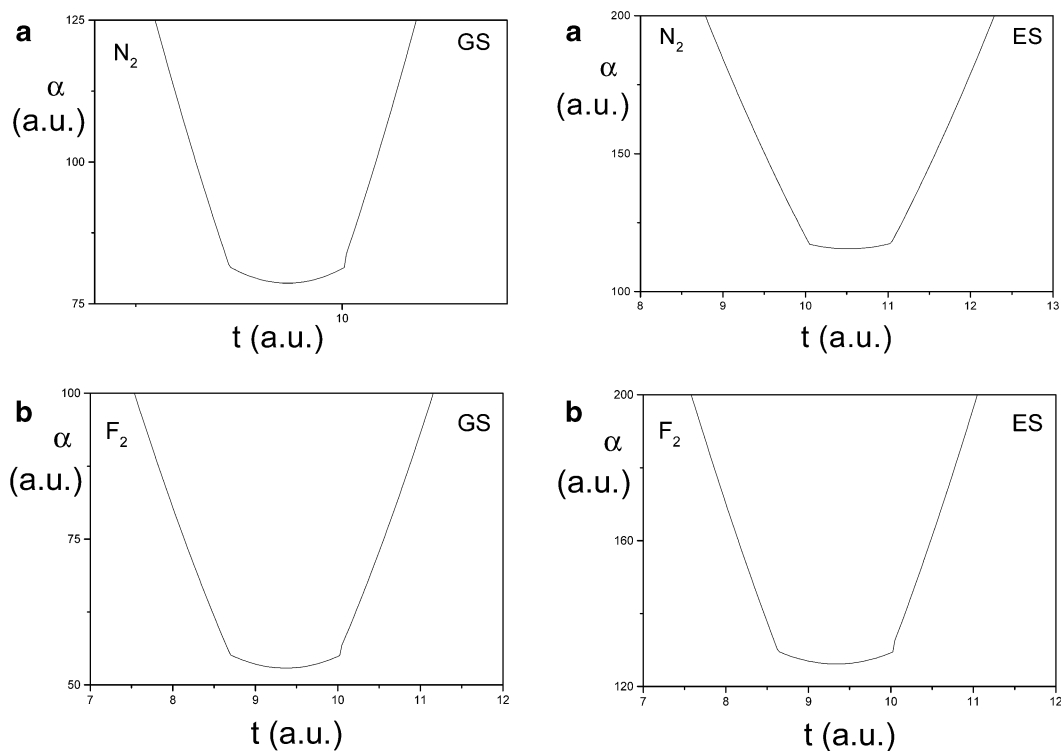


**Figure 2.** (a, left) Time (a.u.) evolution of polarizability ( $\alpha$ , a.u.) during a collision process between a nitrogen molecule in its ground state and a proton. (a, right) Time (a.u.) evolution of polarizability ( $\alpha$ , a.u.) during a collision process between a nitrogen molecule in its first excited state and a proton. (b, left) Time (a.u.) evolution of polarizability ( $\alpha$ , a.u.) during a collision process between a fluorine molecule in its ground state and a proton. (b, right) Time (a.u.) evolution of polarizability ( $\alpha$ , a.u.) during a collision process between a fluorine molecule in its first excited state and a proton.

in CO. Mulliken charges of H and F in HF are 0.5146 and 9.4854, of B and F in BF are 4.7194 and 9.2806, and of C and O in CO are 5.7991 and 8.2009, respectively. For the first excited electronic state, the density profile decreases at the nuclear sites but spreads out more as one goes radially away from the

nuclei. In both states, the electron density of F nuclei in HF, F nuclei in BF, and O nuclei in CO are larger than H nuclei in HF, B nuclei in BF, and C nuclei in CO, respectively.

Figures 3a–c and 4a–c respectively depict the TD hardness and polarizability profiles for protonation considering the attack

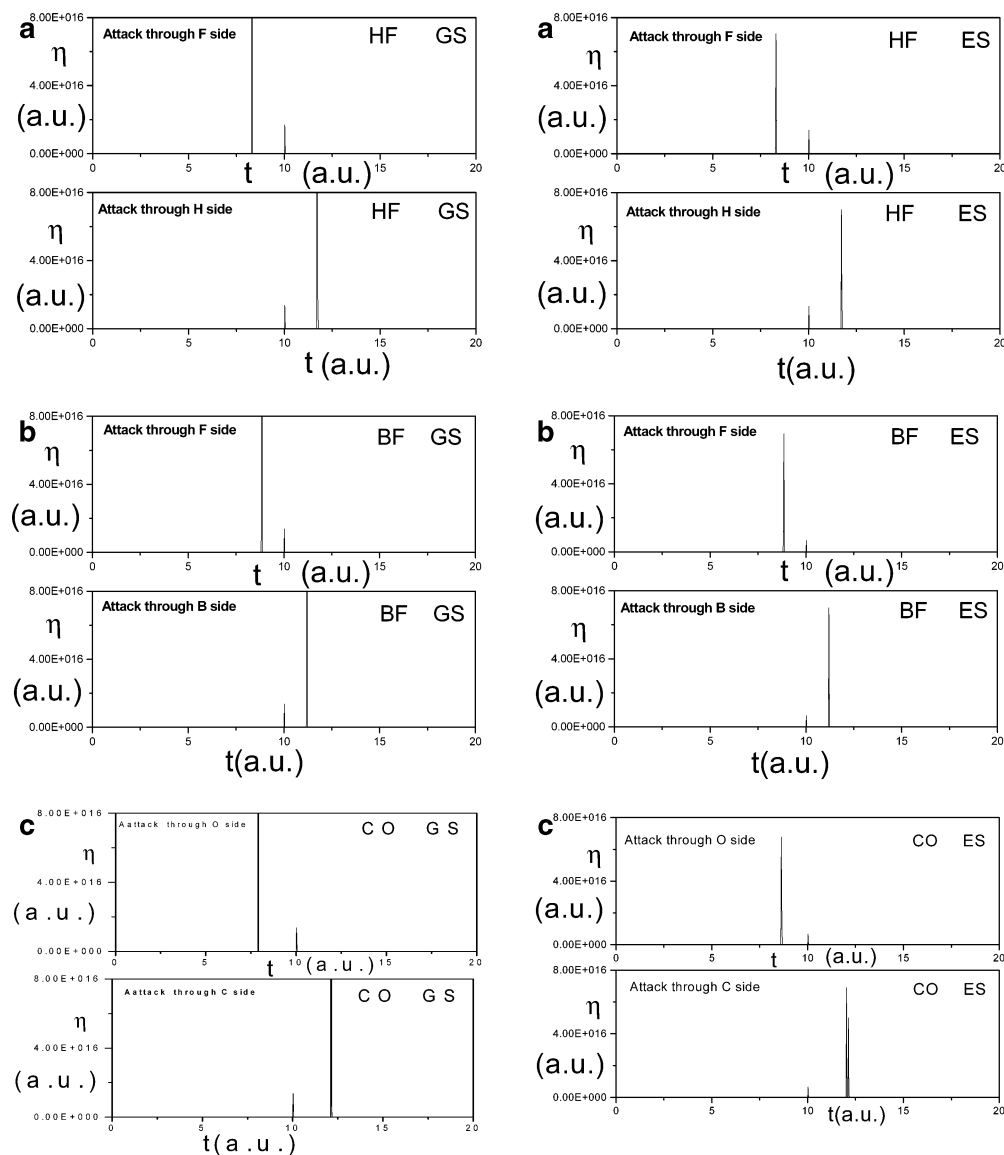


**Figure 3.** (a, left) TD hardness ( $\eta$ , a.u.) profile for the protonation of HF in its ground state considering the attack from both the hydrogen and fluorine sides. (a, right) TD hardness ( $\eta$ , a.u.) profile for the protonation of HF in its first excited state considering the attack from both the hydrogen and fluorine sides. (b, left) TD hardness ( $\eta$ , a.u.) profile for the protonation of BF in its ground state considering the attack from both the boron and fluorine sides. (b, right) TD hardness ( $\eta$ , a.u.) profile for the protonation of BF in its first excited state considering the attack from both the boron and fluorine sides. (c, left) TD hardness ( $\eta$ , a.u.) profile for the protonation of CO in its ground state considering the attack from both the carbon and oxygen sides. (c, right) TD hardness ( $\eta$ , a.u.) profile for the protonation of CO in its first excited state considering the attack from both the carbon and oxygen sides.

from both sides, which is consistent in both the ground and first excited electronic states of the molecules. According to these figures vis-à-vis the MHP and MPP, the F site in HF,<sup>25</sup> F site in BF, and O site in CO are kinetically more favorable to protonation in both electronic states. This explains the laboratory synthesis<sup>52</sup> of isoformyl cation  $\text{HOC}^+$  as well as its presence in dense interstellar clouds<sup>17</sup> such as in the source Sagittarius B2. The proton, being hard, would prefer to attack at the harder F-end in HF, F-end in BF, and O-end in CO to form more stable  $\text{H}_2\text{F}^+$ ,  $\text{HFB}^+$ , and  $\text{HOC}^+$  cations. During excitation,  $\eta_{\text{max}}$  gets smaller and  $\alpha_{\text{min}}$  gets larger when compared to the corresponding values for the ground states, so protonation is less preferable in the excited state than in the ground state. The formation of  $\text{H}_2\text{F}^+$ ,  $\text{HFB}^+$ , and  $\text{HOC}^+$  is thus suggested by both the HSAB principle and Klopman's theory<sup>53</sup> of charge-controlled hard-hard interactions. After formation,  $\text{HOC}^+$  may rearrange itself to generate thermodynamically more stable<sup>53</sup> formyl cation  $\text{HCO}^+$ .

Therefore, with the help of the HSAB principle, we better analyzed the chemical process as well as the regioselectivity. A similar result from the reaction of a proton with  $\text{H}_2$  in ground and excited electronic states as well as with CO in the ground state is published elsewhere.<sup>54</sup>

## V. Concluding Remarks

Quantum fluid density functional theory is useful in understanding the dynamical behavior of chemical reactivity indices during a chemical reaction involving ground and first excited electronic states between protons and molecules. Regioselectivity can be very successfully explained with the help of QFDFT. During chemical processes, hardness is maximized and polarizability is minimized as expected from the principles of maximum hardness and minimum polarizability. In an excited electronic state, a system becomes softer and more polarizable. Because a proton is a hard acid, this fact is a clear-cut signature of the HSAB principle in a dynamical situation.



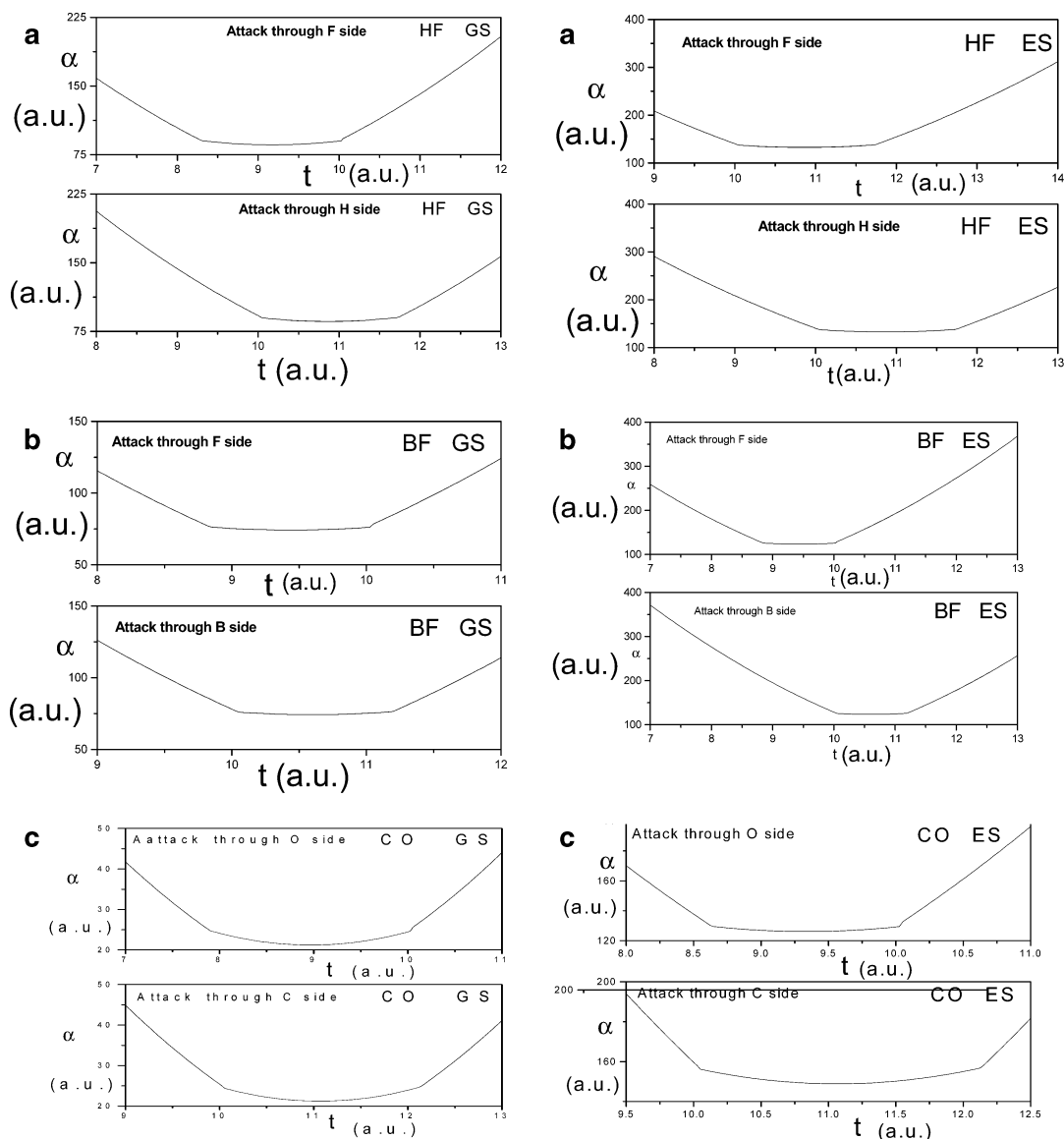


**Figure 4.** (a, left) TD polarizability ( $\alpha$ , a.u.) profile for the protonation of HF in its ground state considering the attack from both the hydrogen and fluorine sides. (a, right) TD polarizability ( $\alpha$ , a.u.) profile for the protonation of HF in its first excited state considering the attack from both the hydrogen and fluorine sides. (b, left) TD polarizability ( $\alpha$ , a.u.) profile for the protonation of BF in its ground state considering the attack from both the boron and fluorine sides. (b, right) TD polarizability ( $\alpha$ , a.u.) profile for the protonation of BF in its first excited state considering the attack from both the boron and fluorine sides. (c, left) TD polarizability ( $\alpha$ , a.u.) profile for the protonation of CO in its ground state considering the attack from both the carbon and oxygen sides. (c, right) TD polarizability ( $\alpha$ , a.u.) profile for the protonation of CO in its first excited state considering the attack from both the carbon and oxygen sides.

**Acknowledgment.** We thank CSIR, New Delhi for financial assistance and the reviewers for constructive criticism.

**Supporting Information Available:** Density profiles of the  $N_2$ ,  $F_2$ , HF, BF, and CO molecules in their ground and first excited electronic states. This material is available free of charge via the Internet at <http://pubs.acs.org>.

## References and Notes

- (1) Kulander, K. C.; Sandhya Devi, K. R.; Koonin, S. E. *Phys. Rev. A* **1982**, *25*, 2968.
- (2) Rudd, M. E.; Kim, Y. K.; Madison, D. H.; Gay, T. J. *Rev. Mod. Phys.* **1992**, *64*, 441.
- (3) Datz, S.; Hippler, R.; Anderson, L. H.; Dittner, P. F.; Knudson, H.; Krasuse, H. F.; Miller, P. D.; Pepniller, P. L.; Rossel, T.; Schuch, R.; Stolterfoht, N.; Yanazaki, Y.; Vane, C. R. *Phys. Rev. A* **1990**, *41*, 3559.
- (4) Runge, K.; Micha, D. A.; Feng, E. Q. *Int. J. Quantum Chem.* **1990**, *24*, 781.
- (5) Deumens, E.; Diz, A.; Taylor, H.; Öhrn, Y. *J. Chem. Phys.* **1992**, *96*, 6820.
- (6) Kimura, M.; Lin, C. D. *Phys. Rev. A* **1986**, *34*, 176.
- (7) Fritsch, W.; Lin, C. D. *J. Phys. B* **1986**, *19*, 2683.
- (8) Singal, R.; Lin, C. D. *J. Phys. B* **1991**, *24*, 251.
- (9) Burgdörfer, J.; Dube, L. J. *Phys. Rev. Lett.* **1984**, *52*, 2225.
- (10) Deb, B. M.; Chattaraj, P. K.; Mishra, S. *Phys. Rev. A* **1991**, *43*, 1248.
- (11) Winter, T. G. *Phys. Rev. A* **1992**, *44*, 4353.
- (12) Doweck, D.; Houver, C. J.; Pommier, J.; Richter, C.; Royer, T.; Anderson, N.; Palsdottir, B. *Phys. Rev. Lett.* **1990**, *64*, 1713.
- (13) Houver, C. J.; Doweck, D.; Richter, C.; Anderson, N. *Phys. Rev. Lett.* **1992**, *68*, 162.
- (14) Cline, R. A.; Westerveld, W. B.; Risley, J. S. *Phys. Rev. A* **1991**, *43*, 1611.
- (15) Rudd, M. E.; Kim, Y. K.; Madison, D. H.; Gallagher, J. W. *Rev. Mod. Phys.* **1985**, *57*, 965.
- (16) *Phase Ion Chemistry*; Bowers, M. T., Ed.; Academic Press: New York, 1979; Vols. 1 and 2.
- (17) Woods, R. C.; Gudemann, C. S.; Dickman, R. L.; Goldsmith, P. F.; Huguenin, G. R.; Irvine, W. M.; Hjalmarson, A.; Nyman, L. A.; Olofsson, H. *Astrophys. J.* **1983**, *270*, 583.
- (18) Pearson, R. G. *Chemical Hardness: Application from Molecules to Solid*; Wiley-VCH: Weinheim, Germany, 1997.

- (19) Sen, K. D.; Mingos, D. M. P. *Chemical Hardness: Structure and Bonding*; Vol. 80; Springer: Berlin, 1993.
- (20) Parr, R. G.; Yang, W. *Density Functional Theory of Atoms and Molecules*; Oxford University Press: Oxford, England, 1989.
- (21) (a) Pearson, R. G. *Hard and Soft Acids and Bases*; Dowden Hutchinson & Ross: Stroudsburg, PA, 1973. (b) Parr, R. G.; Pearson, R. G. *J. Am. Chem. Soc.* **1983**, *105*, 7512.
- (22) Pearson, R. G. *J. Chem. Educ.* **1987**, *64*, 561. Pearson, R. G. *Acc. Chem. Res.* **1993**, *26*, 250.
- (23) (a) Parr, R. G.; Chattaraj, P. K. *J. Am. Chem. Soc.* **1991**, *113*, 1854. (b) Chattaraj, P. K.; Liu, G. H.; Parr, R. G. *Chem. Phys. Lett.* **1995**, *237*, 177. (c) Ayers, P. W.; Parr, R. G. *J. Am. Chem. Soc.* **2000**, *122*, 2010.
- (24) Chattaraj, P. K. *Indian Natl. Sci. Acad. Part A* **1996**, *62*, 513.
- (25) (a) Chattaraj, P. K.; Lee, H.; Parr, R. G. *J. Am. Chem. Soc.* **1991**, *113*, 1855. (b) Chattaraj, P. K.; Schleyer, P. v. R. *J. Am. Chem. Soc.* **1994**, *116*, 1067. (c) Cedillo, A.; Chattaraj, P. K.; Parr, R. G. *Int. J. Quantum Chem. (M. Zerner Special Issue)* **2000**, *77*, 403. (d) Chattaraj, P. K.; Nath, S. *Indian J. Chem., Sect. A* **1994**, *33*, 842.
- (26) (a) Politzer, P. J. *Chem. Phys.* **1987**, *86*, 1072. (b) Ghanty, T. K.; Ghosh, S. K. *J. Phys. Chem.* **1993**, *97*, 4951. (c) Fuentealba, P.; Reyes, O. *J. Mol. Struct.: THEOCHEM* **1993**, *282*, 65. (d) Fuentealba, P.; Simon-Manso, Y. *J. Phys. Chem. A* **1998**, *102*, 2029.
- (27) (a) Chattaraj, P. K.; Sengupta, S. J. *Phys. Chem.* **1996**, *100*, 16126. (b) Ghanty, T. K.; Ghosh, S. K. *J. Phys. Chem.* **1996**, *100*, 12295.
- (28) Pearson, R. G.; Palke, W. E. *J. Phys. Chem.* **1992**, *100*, 16126.
- (29) Galván, M.; Pino, A. D.; Joannopoulos, J. D. *Phys. Rev. Lett.* **1993**, *70*, 21.
- (30) Pal, S.; Vaval, N.; Roy, R. K. *J. Phys. Chem.* **1993**, *97*, 4404.
- (31) (a) Chattaraj, P. K.; Poddar, A. *J. Phys. Chem. A* **1998**, *102*, 9944. Chattaraj, P. K.; Poddar, A. *J. Phys. Chem. A* **1999**, *103*, 1274. Chattaraj, P. K.; Poddar, A. *J. Phys. Chem. A* **1999**, *103*, 8691. (b) Chattaraj, P. K.; Sengupta, S. *J. Phys. Chem. A* **1997**, *101*, 7893. (c) Chattaraj, P. K.; Maiti, B. *J. Am. Chem. Soc.* **2003**, *125*, 2705.
- (32) (a) Hohenberg, P.; Kohn, W. *Phys. Rev. B* **1964**, *136*, 864. (b) Kohn, W.; Sham, L. J. *Phys. Rev. A* **1965**, *140*, 1133.
- (33) (a) Runge, E.; Gross, E. K. U. *Phys. Rev. Lett.* **1984**, *52*, 997. (b) Dhara, A. K.; Ghosh, S. K. *Phys. Rev. A* **1987**, *311*, 47.
- (34) Singh, R.; Deb, B. M. *Phys. Rep.* **1999**, *311*, 47.
- (35) (a) Gunnarsson, O.; Lundqvist, B. I. *Phys. Rev. B* **1976**, *13*, 4274. (b) Ziegler, T.; Rauk, A.; Baerends, E. J. *Theor. Chim. Acta* **1977**, *43*, 261. (c) von Barth, U. *Phys. Rev. A* **1979**, *20*, 1693.
- (36) (a) Theophilou, A. *J. Phys. C* **1979**, *12*, 5419. (b) Hadjisavvas, N.; Theophilou, A. *Phys. Rev. A* **1985**, *32*, 720. (c) Kohn, W. *Phys. Rev. A* **1986**, *34*, 5419. (d) Gross, E. K. U.; Oliveira, L. N.; Kohn, W. *Phys. Rev. A* **1988**, *37*, 2805, 2809. (e) Oliveira, L. N.; Gross, E. K. U.; Kohn, W. *Phys. Rev. A* **1988**, *37*, 2821.
- (37) (a) Berkowitz, M.; Ghosh, S. K.; Parr, R. G. *J. Am. Chem. Soc.* **1985**, *107*, 6811. (b) Ghosh, S. K.; Berkowitz, M. *J. Chem. Phys.* **1985**, *83*, 2976.
- (38) Parr, R. G.; Yang, W. *J. Am. Chem. Soc.* **1984**, *106*, 2976.
- (39) Chattaraj, P. K.; Maiti, B. *J. Phys. Chem. A* **2001**, *105*, 169.
- (40) Fuentealba, P.; Simon-Manso, Y.; Chattaraj, P. K. *J. Phys. Chem. A* **2000**, *122*, 348.
- (41) Deb, B. M.; Chattaraj, P. K. *Phys. Rev. A* **1989**, *39*, 1639.
- (42) Dey, B. K.; Deb, B. M. *Int. J. Quantum Chem.* **1995**, *56*, 707.
- (43) Becke, A. D. *J. Chem. Phys.* **1986**, *84*, 4524.
- (44) Ghosh, S. K.; Deb, B. M. *J. Phys. B* **1994**, *27*, 381.
- (45) Brual, G.; Rothstein, S. M. *J. Chem. Phys.* **1978**, *101*, 7893.
- (46) Chattaraj, P. K.; Sengupta, S. *J. Phys. Chem. A* **1999**, *103*, 6122.
- (47) Madelung, E. Z. *Phys.* **1926**, *40*, 322.
- (48) (a) Deb, B. M.; Ghosh, S. K. *J. Chem. Phys.* **1982**, *77*, 342. (b) Bartolotti, L. J. *Phys. Rev. A* **1982**, *26*, 2243.
- (49) Fuentealba, P. *J. Chem. Phys.* **1995**, *103*, 6571.
- (50) Parr, R. G. *J. Phys. Chem.* **1988**, *92*, 6571.
- (51) Snyder, L. C.; Basch, H. *Molecular Wave Functions and Properties: Tabulated from SCF Calculations in a Gaussian Basis Set*; Wiley & Sons: New York, 1972.
- (52) Gudeman, S. C.; Woods, R. C. *Phys. Rev. Lett.* **1982**, *48*, 1344.
- (53) (a) Oláh, J.; Alsenoy, C. V.; Sannigrahi, A. B. *J. Phys. Chem. A* **2002**, *106*, 3885. (b) Klopman, G. *J. Am. Chem. Soc.* **1968**, *90*, 223. (c) Dixon, D. A.; Komornicki, A.; Kraemer, W. P. *J. Chem. Phys.* **1984**, *81*, 3603.
- (54) Chattaraj, P. K.; Maiti, B. *J. Am. Chem. Soc.* **2003**, *125*, 2705.